

# Early formation of evolved asteroidal crust

James M. D. Day<sup>1</sup>, Richard D. Ash<sup>1</sup>, Yang Liu<sup>2</sup>, Jeremy J. Bellucci<sup>1</sup>, Douglas Rumble III<sup>3</sup>, William F. McDonough<sup>1</sup>, Richard J. Walker<sup>1</sup> & Lawrence A. Taylor<sup>2</sup>

Mechanisms for the formation of crust on planetary bodies remain poorly understood<sup>1</sup>. It is generally accepted that Earth's andesitic continental crust is the product of plate tectonics<sup>1,2</sup>, whereas the Moon acquired its feldspar-rich crust by way of plagioclase flotation in a magma ocean<sup>3,4</sup>. Basaltic meteorites provide evidence that, like the terrestrial planets, some asteroids generated crust and underwent large-scale differentiation processes<sup>5</sup>. Until now, however, no evolved felsic asteroidal crust has been sampled or observed. Here we report age and compositional data for the newly discovered, paired and differentiated meteorites Graves Nunatak (GRA) 06128 and GRA 06129. These meteorites are feldspar-rich, with andesite bulk compositions. Their age of  $4.52 \pm 0.06$  Gyr demonstrates formation early in Solar System history. The isotopic and elemental compositions, degree of metamorphic re-equilibration and sulphide-rich nature of the meteorites are most consistent with an origin as partial melts from a volatile-rich, oxidized asteroid. GRA 06128 and 06129 are the result of a newly recognized style of evolved crust formation, bearing witness to incomplete differentiation of their parent asteroid and to previously unrecognized diversity of early-formed materials in the Solar System.

Formation of crust, the outermost solid shell of a planet, is a fundamental process and its chemical nature is a reflection of the formation, differentiation and cooling history of its parent body. Thus, documenting causes of lithological diversity in crustal materials is critical for understanding early Solar System processes and planetary evolution. Knowledge regarding initial formation of planetary crust is largely based on data gleaned from the oldest preserved crustal rock and mineral remnants from Earth (<4.4 Gyr; refs 6, 7), the Moon (~4.4 Gyr; ref. 8), Mars (>4.0 Gyr; ref. 9) and achondrite meteorites ( $\leq 4.56$  Gyr; ref. 10). These materials record crustal formation processes that were demonstrably diverse among these bodies.

GRA 06128 and 06129 (hereafter referred to as GRA 06128/9) are paired achondritic meteorites recovered from the same Antarctic ice-field. The meteorites consist largely of sodium-rich plagioclase (>75%), with olivine, two pyroxenes, phosphates and sulphides. They have andesite to trachy-andesite bulk compositions (Fig. 1a; see Methods and Supplementary Information). Major- and trace-element compositions of silicate minerals are uniform within and between the two meteorites. Minerals are compositionally unzoned and major silicate phases have variable ranges of grain size (diameter <0.1 to >0.5 mm). Co-existing augite and orthopyroxene yield equilibration temperatures of ~800°C. Oligoclase crystals have large positive Eu anomalies, and merrillite and chlorapatite have elevated rare-earth element (REE) abundances, relative to other minerals in the meteorites. Consequently, the estimated bulk REE composition of GRA 06128/9, determined by modal recombination, is dominated by feldspar for Eu and phosphates for the other REEs (Fig. 1b). The meteorites are enriched to only moderately depleted in volatile elements (for example

K, Na, S, Rb, Cl, Pb) relative to chondrites, and were formed at an oxygen fugacity close to the iron-wüstite +2 buffer (ref. 11).

Although GRA 06128/9 had an igneous origin, they have also been thermally metamorphosed and partially brecciated. Both meteorites possess granoblastic textures, 120° triple junctions between coexisting silicates, polysynthetic twinning in plagioclase and pentlandite-troilite exsolution from a monosulphide solid solution. These features are consistent with slow cooling and partial re-equilibration. Using pyroxene exsolution lamellae, it has been estimated that GRA 06128/9 formed close to the surface (at depths of 15–20 m) of their

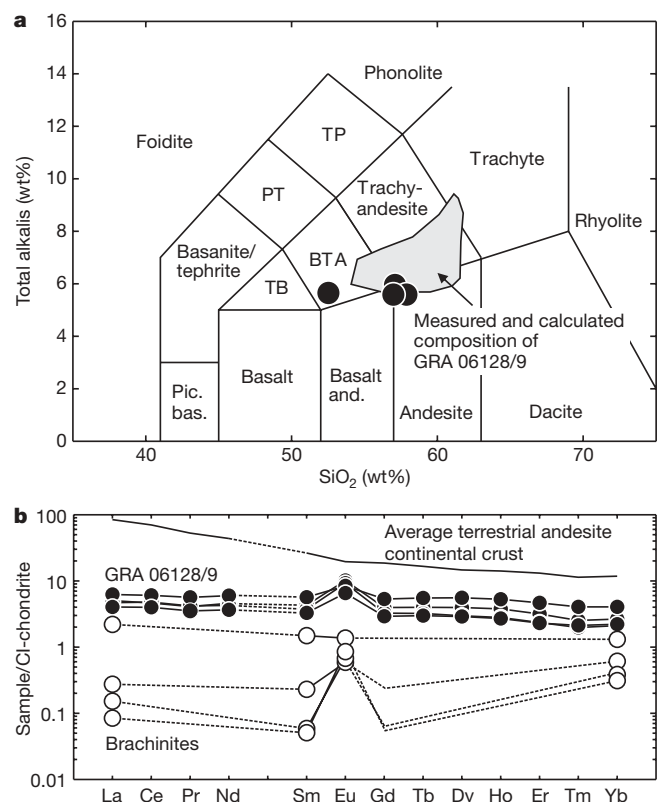


**Figure 1 | Bulk composition of the GRA 06128/9 achondrite meteorites.** **a**, Plot of total alkalis ( $\text{Na}_2\text{O}$  and  $\text{K}_2\text{O}$ ) versus silica, showing multiple measurements (filled circles) and calculated compositions (grey area) of the GRA 06128/9 achondrite meteorites. Calculated compositions are based on the variability in modal mineralogy and mineral major element compositions (Supplementary Information). Abbreviations: TP, trachy-phonolite; PT, phono-tephrite; TB, trachy-basalt; BTA, basaltic trachy-andesite; Pic. bas., picro-basalt; Basalt and., basaltic andesite. **b**, Measured REE patterns for the GRA 06128/9 meteorites. Shown are data for the average terrestrial continental crust<sup>1</sup> and for the brachinites, Brachina, ALH 84025 and EET 99402/407 (ref. 26).

<sup>1</sup>Department of Geology, University of Maryland, College Park, Maryland 20742, USA. <sup>2</sup>Department of Earth and Planetary Sciences, Planetary Geosciences Institute, University of Tennessee, Knoxville, Tennessee 37996, USA. <sup>3</sup>Geophysical Laboratory, Carnegie Institution for Science, Washington DC 20015, USA.

**Table 1 | Three oxygen isotope data for GRA 06128 and GRA 06129**

| Sample, specific number | $\delta^{17}\text{O}$ (‰) | $\delta^{18}\text{O}$ (‰) | $\Delta^{17}\text{O}$ (‰) |
|-------------------------|---------------------------|---------------------------|---------------------------|
| GRA 06128, 22           | 2.457                     | 5.052                     | -0.200                    |
| GRA 06128, 22           | 2.330                     | 4.822                     | -0.207                    |
| GRA 06128 average       | $2.394 \pm 0.090$         | $4.937 \pm 0.162$         | $-0.204 \pm 0.005$        |
| GRA 06129, 9            | 2.421                     | 4.968                     | -0.192                    |
| GRA 06129, 9            | 2.334                     | 4.777                     | -0.179                    |
| GRA 06129 average       | $2.378 \pm 0.062$         | $4.873 \pm 0.135$         | $-0.186 \pm 0.009$        |

parent body<sup>12</sup>. This conclusion is consistent with an origin as evolved crustal material.

Oxygen isotopes (as  $\Delta^{17}\text{O}$  values) provide a means to genetically link Solar System materials (ref. 13;  $\Delta^{17}\text{O}$  notation is defined in Methods). The  $\Delta^{17}\text{O}$  values for multiple pieces of GRA 06128/9 average  $-0.195 \pm 0.012$ ‰ (Fig. 2; Table 1). This isotopic composition is different from most known differentiated bodies, including the Earth, Moon and Mars.

The mean  $^{207}\text{Pb}$ - $^{206}\text{Pb}$  age determined for chlorapatite in GRA 06128/9 is  $4.517 \pm 0.060$  Gyr ( $2\sigma$ ; Supplementary Methods). The mean age for merrillite crystals is identical within the greater uncertainty. Since  $^{207}\text{Pb}$ - $^{206}\text{Pb}$  ages reflect the time of cessation of Pb diffusion (ref. 14), the measured phosphate ages probably reflect closure temperatures subsequent to the metamorphic event recorded from pyroxene thermometry ( $\leq 800$  °C). Assuming that diffusion characteristics are similar to those of terrestrial phosphates, the closure temperature of Pb in merrillite and chlorapatite in GRA 06128/9 is  $\sim 500$  °C (ref. 14). Thus, the phosphate age of GRA 06128/9 demonstrates that crystallization, thermal metamorphism and cooling below 500 °C occurred within  $\sim 100$  Myr of the formation of the Solar System at  $\sim 4.567$  Gyr ago<sup>15</sup>. These ages can be used to argue against an origin on any major planetary body, including Venus or Mercury. The average age of the crust on Venus is estimated to be  $< 1$  Gyr (ref. 16), and present knowledge of Mercury suggests it is highly reduced, with a crust that is younger than 4.4 Gyr (ref. 17).

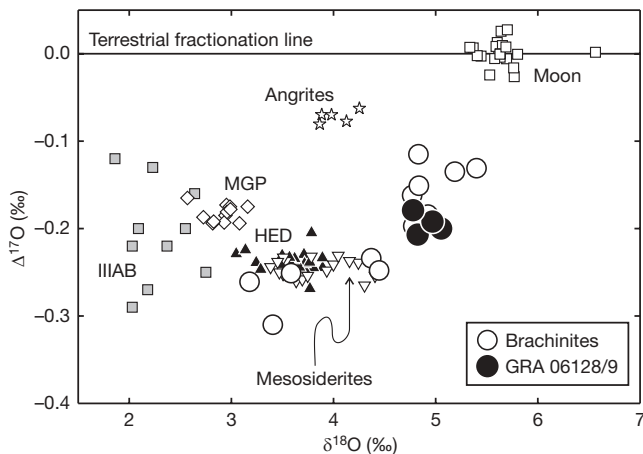


**Figure 2 |  $\delta^{18}\text{O}$ - $\Delta^{17}\text{O}$  plot for GRA 06128/9 versus achondrite meteorites and lunar and terrestrial materials.** MGP, main group pallasites (open diamonds); IIIAB, IIIAB iron meteorites (filled grey squares); HED, howardite-eucrite-diogenite meteorites (filled triangles). The GRA 06128/9 meteorites have oxygen isotope compositions most similar to brachinites. Published data are from refs 5, 32 and references therein. Error bars for data are smaller than symbols.

**Table 2 | Whole-rock highly siderophile element data with initial Os isotopic compositions at 4.52 Gyr**

| Sample    | Specific number | Mass (g) | Os (p.p.b.) | Ir (p.p.b.) | Ru (p.p.b.) | Pt (p.p.b.) | Pd (p.p.b.) | Re (p.p.b.) | $^{187}\text{Os}/^{188}\text{Os}_m$ | 2s.e.   | $^{187}\text{Re}/^{188}\text{Os}$ | 2s.e. | $^{187}\text{Os}/^{188}\text{Os}_i$ | 2s.e.  |
|-----------|-----------------|----------|-------------|-------------|-------------|-------------|-------------|-------------|-------------------------------------|---------|-----------------------------------|-------|-------------------------------------|--------|
| GRA 06128 | 22              | 0.21     | 175.1       | 78.58       | 301.4       | 125.9       | 53.55       | 16.06       | 0.13100                             | 0.00009 | 0.442                             | 0.007 | 0.0964                              | 0.0015 |
| GRA 06129 | 9               | 0.26     | 265.0       | 95.56       | 378.1       | 143.0       | 54.93       | 24.30       | 0.13117                             | 0.00005 | 0.442                             | 0.007 | 0.0966                              | 0.0015 |
| Brachina  | USNM 535L       | 0.06     | 156.0       | 142.6       | 228.9       | 110.6       | 67.45       | 10.12       | 0.12041                             | 0.00014 | 0.312                             | 0.005 | 0.0960                              | 0.0011 |

m, measured; i, initial; s.e., standard error.

Taken with the oxygen isotope evidence, we conclude that GRA 06128/9 originated on an asteroid.

Owing to their tendency to strongly partition into metal relative to silicate, the highly siderophile elements (HSE; including Re, Os, Ir, Ru, Pt and Pd) are important recorders of primary planetary differentiation. Concentrations of the HSE in bulk samples of GRA 06128/9 are elevated, in some cases within a factor of two or three of chondritic abundances (Table 2; Fig. 3). These results demonstrate that a metallic core had not segregated before generation of the GRA 06128/9 parental melts. Some of the HSE are fractionated relative to one another in GRA 06128/9. These fractionated HSE compositions could not have been incorporated into the rock via the impact of any known chondritic or metal-rich meteorite material. Nor can they be explained through terrestrial weathering processes. Although the meteorites are weathered (Supplementary Information), laser ablation inductively coupled plasma-mass spectrometry analysis of unaltered sulphides and FeNi metal in the meteorites reveals that the HSE are hosted almost entirely within these primary magmatic phases (Fig. 3). Furthermore, the calculated initial  $^{187}\text{Os}/^{188}\text{Os}$  ratio for the GRA 06128/9 meteorites ( $0.096 \pm 0.001$ ) is within error of the initial Solar System value, inconsistent with disturbance of the  $^{187}\text{Re}$ - $^{187}\text{Os}$  system and consistent with formation via early partial melting of an undifferentiated parent body.

The formation mechanism for GRA 06128/9 was evidently unique among known achondrites. Plagioclase-rich lunar ferroan anorthosites are considered to represent flotation cumulates from a large-scale magma ocean melting event<sup>3,4</sup>. The elevated abundances of the HSE, however, argue against this mode of origin for the GRA 06128/9 meteorites, as  $> 50\%$  melting of the silicate fraction of an asteroid would lead to formation of a gravitationally separated metal-liquid core (ref. 18). Consequently, large-scale differentiation leads to marked depletion of HSE in the silicate portion of the body. For example, lunar and terrestrial crustal rocks respectively contain less than  $\sim 0.02$  ng g<sup>-1</sup> and  $\sim 0.04$  ng g<sup>-1</sup> Os (refs 1, 19), as compared with  $\sim 200$  ng g<sup>-1</sup> Os for GRA 06128/9. Furthermore, HED meteorites, which are considered to derive from the asteroid 4 Vesta (mean diameter  $\sim 530$  km) and are probably the result of a large-scale magma ocean melting event<sup>5</sup>, also have very low abundances of the HSE<sup>20</sup>—compositions at odds with those of GRA 06128/9.

It has been demonstrated that quartz-normative andesite compositions like that of GRA 06128/9 can be generated by partial melting of volatile-rich chondritic precursors (see, for example, ref. 21). These studies have shown that partial melting of an olivine-rich lithology in the forsterite-anorthite-quartz system occurs at the peritectic point, resulting in a melt that contains  $> 50\%$  plagioclase<sup>22</sup>. Furthermore, Na-rich compositions lower liquidus temperatures by up to 100 °C and shift the initial melt compositions to even higher abundances of feldspar<sup>23,24</sup>. These experimental constraints, together with the major-, trace-element and mineralogical data for GRA 06128/9, indicate that they most probably crystallized from magma generated by partial melting of a primitive chondritic source.

The formation of GRA 06128/9 by partial melting and melt segregation of a largely undifferentiated body implies the possibility of a complementary ultramafic residue or cumulate. There are numerous mafic and ultramafic achondrite meteorites in the terrestrial collection, of which the brachinites possess the most complementary characteristics to the GRA 06128/9 meteorites, including overlapping  $\Delta^{17}\text{O}$  values (Fig. 2; ref. 25). The significant O isotope variability present in brachinites ( $\Delta^{17}\text{O} = -0.15$  to  $-0.31$ ‰) has been attributed to partial or incomplete melting of their primitive

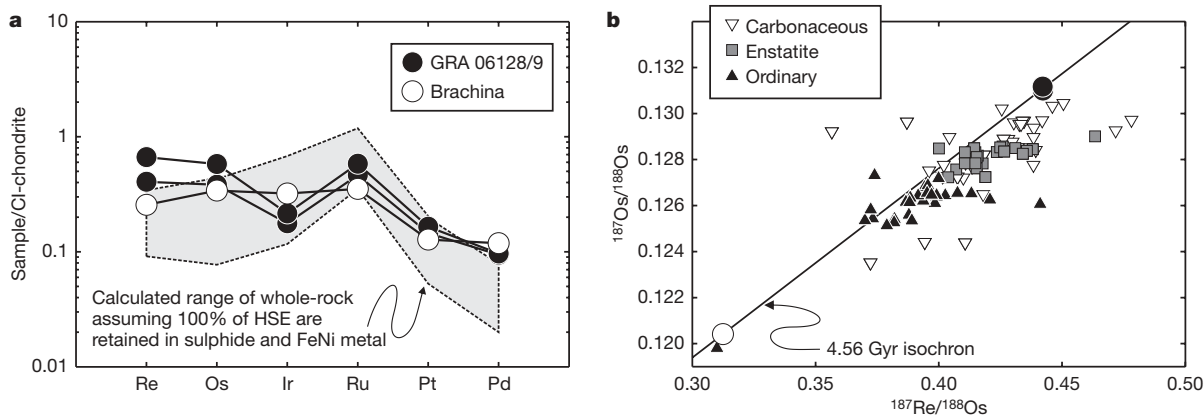


**Figure 3 | Highly siderophile element and Re–Os isotope systematics of GRA 06128/9 and Brachina.** **a**, Measured HSE patterns for GRA 06128/9 and Brachina showing significant fractionation of Ir, Pt and Pd from Re, Os and Ru in the meteorites relative to CI chondrite (Orgueil). Also shown is the calculated whole-rock compositional field (shaded) for GRA 06128/9 using measured modal abundances and HSE compositions of pentlandite/FeNi metal and FeS in the meteorites (Supplementary Information). These calculated estimates are in broad agreement with measured whole-rock values, indicating that HSE are dominantly hosted within sulphide and FeNi

metal. **b**,  $^{187}\text{Re}/^{188}\text{Os}$ – $^{187}\text{Os}/^{188}\text{Os}$  diagram for GRA 06128/9 and Brachina versus chondritic meteorites. GRA 06128/9 plot to elevated values relative to all chondrite groups in  $^{187}\text{Re}/^{188}\text{Os}$ – $^{187}\text{Os}/^{188}\text{Os}$  space. Brachina (open circle) has present-day sub-chondritic  $^{187}\text{Os}/^{188}\text{Os}$ . GRA 06128/9 (filled circles) and Brachina plot along a  $\sim 4.56$  Gyr isochron, with an  $^{187}\text{Os}/^{188}\text{Os}$  value close to the Solar System initial value, which passes through the field of chondritic meteorite data. Normalization and chondrite data are from ref. 33. Error bars for GRA 06128/9 and Brachina data are smaller than symbols.

parent body<sup>26,27</sup>, consistent with the projected parent body for GRA 06128/9. Further, Brachina (the ‘type’ for brachinites) has fractionated HSE, sub-chondritic measured  $^{187}\text{Os}/^{188}\text{Os}$  (0.1204; versus 0.1311 for GRA 06128/9) and a depleted REE pattern, features that are complementary if brachinites represent melt residues to the GRA 06128/9 meteorites (Figs 1 and 3). These characteristics are consistent with an origin as rocks that did not experience metal–silicate equilibration, but underwent partial melting processes broadly complementary to those required for GRA 06128/9. All of these characteristics provide possible evidence that GRA 06128/9 are either genetically related to the brachinites or derive from a parent body with a similar melting history.

Fractionation of the HSE in GRA 06128/9 can be potentially explained by sulphide segregation. The HSE can be fractionated via removal of a sulphide melt from a crystalline monosulphide solid solution in the terrestrial mantle<sup>28</sup>. Similar styles of fractionation of the HSE between GRA 06128/9 and terrestrial ores may implicate this type of process as acting during generation of the GRA 06128/9 parental melts (see Supplementary Discussion).

It has been previously demonstrated that melting and metamorphism of asteroid parent bodies were unlikely to have occurred through impact-related heating, which has been shown to be a highly inefficient process<sup>29</sup>. This conclusion is supported by the lack of evidence for significant impactor contributions to the HSE inventories of the GRA 06128/9 meteorites; energy released from initial accretion of the parent body, or through decay of short-lived radionuclides (for example,  $^{26}\text{Al}$ ), represent more viable heat sources. Constraints on the size of the parent body of the GRA 06128/9 meteorites can only be loosely applied. On asteroids  $<100$  km in radius, it is likely that volatile-rich, low-density melts such as GRA 06128/9 would exceed escape velocities through explosive pyroclastic volcanism and be lost to space<sup>30</sup>. Thus, GRA 06128/9 could have originated either via extrusion from a large ( $>100$  km radius) asteroid or emplaced intrusively on a body of undetermined size.

Remote sensing of asteroids shows that, where detected, the preponderance of crust is basaltic. This is also true for the terrestrial planets and the asteroid 4 Vesta. Feldspar-rich crust is not uncommon, with the Moon’s crust and Earth’s continental crust being feldspar-rich. Feldspar does not have a strong spectral wavelength absorption in the near-infrared, but its high albedo is a diagnostic feature, and a number of E-type asteroids have been detected in the asteroid belt with this characteristic<sup>31</sup>. These asteroids may also have a

significant sulphide component<sup>31</sup>. The presence of E-type asteroids implies that evolved crust may be extensive on some of these bodies. So far, however, only one planet has been found to have a major andesite crust component, namely Earth. It has been argued that, to generate andesite crust, a significant volatile component is required in the mantle of the parent body<sup>2</sup>. On Earth, this is achieved through recycling of water into subduction zones<sup>1</sup>. The GRA 06128/9 meteorites require early partial melting of primitive, volatile-rich source regions in an asteroidal body that did not suffer extensive planetary differentiation, and thus point to an entirely new mode of generation of andesite crust compositions.

## METHODS SUMMARY

For mineralogical characterization we used an SX50 electron microprobe and New Wave Research UP213 (213 nm) laser-ablation (LA) system coupled to a ThermoFinnigan Element 2 inductively coupled plasma-mass spectrometer (ICP-MS).  $^{207}\text{Pb}$ – $^{206}\text{Pb}$  ages were obtained via LA-ICP-MS and were corrected for mass fractionation using an exponential fractionation law by means of bracketing the phosphate analyses with standard reference materials (SRMs: NIST 610, NIST 612, BCR-2g). Ratios of  $^{207}\text{Pb}/^{206}\text{Pb}$  for each SRM were used to calculate the fractionation factor ( $\alpha$ ). Differences in  $\alpha$  between the three SRMs had a negligible effect on calculated ages. Os isotopic and platinum-group elemental abundance measurements were made using isotope dilution and solvent extraction/anion exchange purification methodologies. Os isotopes and concentrations were measured via thermal ionization mass spectrometry, and Ir, Ru, Pt, Pd and Re abundances were measured using solution ICP-MS. Oxygen isotope analysis was performed via laser fluorination of pre-leached powder whole-rock aliquots stripped of magnetic minerals. Standardization of delta values was achieved by comparison with the Gore Mountain garnet standard, USNM 107144, analysed during every analytical session.

**Full Methods** and any associated references are available in the online version of the paper at [www.nature.com/nature](http://www.nature.com/nature).

Received 26 May; accepted 17 November 2008.

1. Rudnick, R. L. & Gao, S. in *The Crust* (ed. Rudnick, R. L.) Vol. 3, *Treatise on Geochemistry* (eds Holland, H. D. & Turekian, K. K.) 1–64 (Elsevier-Pergamon, 2003).
2. Campbell, I. H. & Taylor, S. R. No water, no granites — no oceans, no continents. *Geophys. Res. Lett.* **10**, 1061–1064 (1985).
3. Wood, J. A., Dickey, J. S., Marvin, U. B. & Powell, B. N. Lunar anorthosites and a geophysical model of the Moon. *Proc. Apollo 11 Lunar Sci. Conf.* 965–988 (1970).
4. Smith, J. A. *et al.* Petrologic history of the Moon inferred from petrography, mineralogy, and petrogenesis of Apollo 11 rocks. *Proc. Apollo 11 Lunar Sci. Conf.* 1149–1162 (1970).

5. Greenwood, R. C., Franchi, I. A., Jambon, A. & Buchanan, P. C. Widespread magma oceans on asteroidal bodies in the early Solar System. *Nature* **435**, 916–918 (2005).
6. Bowring, S. A. & Williams, I. S. Priscoan (4.00–4.03 Ga) orthogneiss from northwestern Canada. *Contrib. Mineral. Petrol.* **134**, 3–16 (1999).
7. Wilde, S. A., Valley, J. W., Peck, W. H. & Graham, C. M. Evidence from detrital zircons for the existence of continental crust and oceans on the Earth 4.4 Gyr ago. *Nature* **409**, 175–178 (2001).
8. Carlson, R. W. & Lugmair, G. The age of ferroan anorthosite 60025: Oldest crust on a young Moon? *Earth Planet. Sci. Lett.* **90**, 119–130 (1988).
9. Ash, R. D., Knott, S. F. & Turner, G. A 4-Gyr shock age for a martian meteorite and implications for the cratering history of Mars. *Nature* **380**, 57–59 (1996).
10. Mittlefehldt, D. W., McCoy, T. J., Goodrich, C. A. & Kracher, A. in *Planetary Materials* (ed. Papike, J. J.) Ch. 4 (Mineralogical Society of America, 1998).
11. Shearer, C. K. et al. GRA 06129: A meteorite from a new asteroidal geochemical reservoir or Venus? *Lunar Planet. Sci. Conf. Abstr. XXXIX*, 1825 (2008).
12. Mikouchi, T. & Miyamoto, M. Mineralogy and pyroxene cooling rate of unique achondrite meteorite GRA 06129. *Lunar Planet. Sci. Conf. Abstr. XXXIX*, 2297 (2008).
13. Clayton, R. N. Oxygen isotopes in meteorites. *Annu. Rev. Earth Planet. Sci.* **21**, 115–149 (1993).
14. Cherniak, D. J., Landrod, W. A. & Ryerson, F. J. Lead diffusion in apatite and zircon using ion implantation and Rutherford back-scattering techniques. *Geochim. Cosmochim. Acta* **55**, 1663–1673 (1991).
15. Amelin, Y., Krot, A. N., Hutcheon, I. D. & Ulyanov, A. A. Lead isotopic ages of chondrules and calcium-aluminium-rich inclusions. *Science* **297**, 1678–1683 (2002).
16. Strom, R. G., Schaber, G. G. & Dawson, D. D. The global resurfacing of Venus. *J. Geophys. Res.* **99** (E5), 10899–10926 (1994).
17. Taylor, G. J. & Scott, E. R. D. in *Meteorites, Comets, and Planets* (ed. Davis, A. M.) Vol. 1, *Treatise on Geochemistry* (eds Holland, H. D. & Turekian, K. K.) 477–486 (Elsevier-Pergamon, 2003).
18. Taylor, G. J. Core formation in asteroids. *J. Geophys. Res.* **97**, 717–726 (1992).
19. Day, J. M. D., Pearson, D. G. & Taylor, L. A. Highly siderophile element constraints on accretion and differentiation of the Earth-Moon system. *Science* **315**, 217–219 (2007).
20. Bircck, J.-L. & Allègre, C. J. Contrasting Re/Os magmatic fractionation in planetary basalts. *Earth Planet. Sci. Lett.* **124**, 139–148 (1994).
21. Jurewicz, A. J. G., Mittlefehldt, D. W. & Jones, J. H. Experimental partial melting of the Allende (CV) and Murchison (CM) chondrites and the origin of asteroidal basalt. *Geochim. Cosmochim. Acta* **57**, 2123–2139 (1995).
22. Morse, S. A. *Basalts and Phase Diagrams* (Springer, 1980).
23. Tuttle, O. F. & Bowen, N. L. Origin of granite in the light of experimental studies in the system NaAlSi<sub>3</sub>O<sub>8</sub>-KAlSi<sub>3</sub>O<sub>8</sub>-SiO<sub>2</sub>-H<sub>2</sub>O. *Geol. Soc. Am. Mem.* **74**, 153p (1958).
24. Kushiro, I. On the nature of silicate melt and its significance in magma genesis; regularities in the shift of the liquidus boundaries involving olivine, pyroxene, and silica minerals. *Am. J. Sci.* **275**, 411–431 (1975).
25. Ziegler, R. A. et al. Petrology, geochemistry and likely provenance of unique achondrite Graves Nunatak 06128. *Lunar Planet. Sci. Conf. Abstr. XXXIX*, 2456 (2008).
26. Mittlefehldt, D. W., Bogard, D. D., Berkley, J. L. & Garrison, D. H. Brachinites: Igneous rocks from a differentiated asteroid. *Meteorit. Planet. Sci.* **38**, 1601–1625 (2003).
27. Rumble, D., Irving, A. J., Bunch, T. E., Wittke, J. H. & Kuehner, S. M. Oxygen isotopic and petrological diversity among Brachinites NWA 4872, NWA 4874, NWA 4882 and NWA 4969: How many ancient parent bodies? *Lunar Planet. Sci. Conf. Abstr. XXXIX*, 1974 (2008).
28. Bockrath, C., Ballhaus, C. & Holzheid, A. Fractionation of the platinum-group elements during mantle melting. *Science* **305**, 1951–1953 (2004).
29. Keil, K., Stöffler, D., Love, S. G. & Scott, E. R. D. Constraints on the role of impact heating and melting in asteroids. *Meteorit. Planet. Sci.* **32**, 349–363 (1997).
30. Wilson, L. & Keil, K. Consequences of explosive eruptions on small solar system bodies: The case of the missing basalts on the aubrite parent body. *Earth Planet. Sci. Lett.* **140**, 191–200 (1991).
31. Clark, B.-E. et al. E-type asteroid spectroscopy and compositional modelling. *J. Geophys. Res.* **109**, doi:10.1029/2003JE002200 (2004).
32. Spicuzza, M. J., Day, J. M. D., Taylor, L. A. & Valley, J. W. Oxygen isotope constraints on the origin and differentiation of the Moon. *Earth Planet. Sci. Lett.* **253**, 254–265 (2007).
33. Horan, M. F., Walker, R. J., Morgan, J. W., Grossman, J. N. & Rubin, A. E. Highly siderophile elements in chondrites. *Chem. Geol.* **196**, 27–42 (2003).

**Supplementary Information** is linked to the online version of the paper at [www.nature.com/nature](http://www.nature.com/nature).

**Acknowledgements** We thank the ANSMET 2006/2007 field team, the Meteorite Working Group and the Smithsonian Institution of Washington for collection and provision of the GRA 06128/9 and Brachina meteorites. D. Mittlefehldt and R. Greenwood provided reviews that improved the quality of this paper. A. Patchen and P. Piccoli provided assistance with electron microprobe analysis. Portions of this study were supported by the NASA Cosmochemistry Program: NNX07AM29G (R.J.W.), NNX08AH76G (W.F.M.), NNG05GG03G (L.A.T.).

**Author Contributions** All authors participated in data collection and interpretation and commented on the manuscript. J.M.D.D led the project and wrote the paper.

**Author Information** Reprints and permissions information is available at [www.nature.com/reprints](http://www.nature.com/reprints). Correspondence and requests for materials should be addressed to J.M.D.D. (jamesday@umd.edu).

## METHODS

Mineralogical investigations of polished thick and thin sections of GRA 06128 (sub-sections 42 and 51) and GRA 06129 (22 and 25) were performed using a Cameca SX50 electron microprobe analyser<sup>34</sup> (EMPA; University of Tennessee). Concentrations of minor and trace elements were determined in minerals using a New Wave Research UP213 (213 nm) laser-ablation system coupled to a ThermoFinnigan Element 2 ICP-MS (University of Maryland). Minerals were analysed using individual spots with a 15–80  $\mu\text{m}$  diameter, a laser repetition rate of 7 Hz and a photon fluence of 2–2.5  $\text{J cm}^{-2}$ . Th/ThO production was  $\sim 0.07\%$  for all analytical sessions. Backgrounds on the ICP-MS sample gas were collected for  $\sim 20$  s followed by  $\sim 40$  s of laser ablation of the sample. Washout time between analyses was  $>2$  min. Data were collected in time-resolved mode so that effects of inclusions, mineral zoning and laser beam penetration could be evaluated. The NIST 610 glass standard was used for calibration of relative element sensitivities. Replicate LA-ICP-MS analyses of the BIR-1g glass standard run at intervals during analytical sessions yielded an external precision of better than 3% ( $1\sigma$  relative standard deviation) for all measured element compositions of silicates and phosphates. Replicate LA-ICP-MS analyses of the University of Toronto JB Sulphide standard run at intervals during analysis of sulphides yielded an external precision of better than 1% ( $1\sigma$  relative standard deviation) for highly siderophile element abundances.

$^{207}\text{Pb}$ – $^{206}\text{Pb}$  ages were obtained using the same laser and mass spectrometer settings as those for minerals and glasses analysed by LA-ICP-MS. Chlorapatite and merrillite were measured because the high concentrations of U (0.1–3 p.p.m.) make them suitable for LA-ICP-MS  $^{207}\text{Pb}$ – $^{206}\text{Pb}$  dating. All data reduction was made offline using Microsoft Excel. Background Pb signals were taken on mass, and subtracted from each isotopic measurement during ablation. Each ratio was determined using the background corrected Pb isotopic measurements. The average and  $2\sigma_{\text{mean}}$  of the background corrected ratios, after ratios outside  $3\sigma$  were discarded, were used to determine the age and error for each phosphate. An exponential fractionation law was used to correct for mass fractionation by means of bracketing the phosphate analyses with standard reference materials (SRM: NIST 610, NIST 612, BCR-2g). Ratios of  $^{207}\text{Pb}/^{206}\text{Pb}$  for each SRM were used to calculate the fractionation factor ( $\alpha$ ; ref. 35). Differences in  $\alpha$  between the three SRMs had a negligible effect on calculated ages. The  $^{207}\text{Pb}$ – $^{206}\text{Pb}$  ages were calculated using Isoplot/Ex (ref. 36).

Fused-bead major element concentrations were analysed using the CAMECA SX-50 EMPA and protocols for glass analyses outlined in ref. 34. Minor- and trace-element concentrations were measured on the same beads using LA-ICP-MS protocols outlined above, with 150- $\mu\text{m}$  raster paths and obtaining 20 s of background and  $\sim 60$  s of analysis. Os isotopic and platinum-group elemental analyses were performed at the University of Maryland using protocols outlined in Supplementary Information. Isotopic compositions of Os were measured in negative ion mode by thermal ionization mass spectrometry. Re, Pd, Pt, Ru and

Ir were measured using an Aridus desolvating nebuliser coupled to an Element 2 ICP-MS in low-resolution mode. External precision for  $^{187}\text{Os}/^{188}\text{Os}$ , determined via measurement of standards bracketed with the meteorite samples, was 2.5‰ ( $2\sigma$ ). External reproducibility on PGE analyses using the Element 2 was better than 0.5% for 0.1 p.p.b. solutions and 0.3% for 1 p.p.b. solutions. Total procedural blanks run with the samples had an average  $^{187}\text{Os}/^{188}\text{Os}$  isotope composition of  $0.1448 \pm 0.0024$ , with average concentrations of 1.5 pg (Re), 37 pg (Pd), 20 pg (Pt), 5 pg (Ru), 2 pg (Ir) and  $<1$  pg (Os); blank corrections were negligible.

Oxygen isotope analyses were performed at the Geophysical Laboratory, Carnegie Institution for Science and are reported in  $\delta^{18}\text{O}$ ,  $\delta^{17}\text{O}$  ( $\delta^X\text{O}_n$  is the per mil (‰) deviation of  $^X\text{O}/^{16}\text{O}$  in  $n$  from the international standard (std) V-SMOW given by the relationship:  $\delta^X\text{O}_n = 1,000 \times ((^X\text{O}/^{16}\text{O}_n) / (^X\text{O}/^{16}\text{O}_{\text{std}}) - 1)$ , where  $X$  is either 17 or 18 and  $n$  represents the unknown) and  $\Delta^{17}\text{O}$  notation, which represents deviations from the terrestrial fractionation line ( $\lambda = 0.526$  (ref. 37);  $\Delta^{17}\text{O} = 1,000 \ln((\delta^{17}\text{O}/1,000) + 1) - 0.526 \times 1,000 \ln((\delta^{18}\text{O}/1,000) + 1)$ ) (after ref. 38). The value of 0.526 was obtained by linear regression of linearized values for  $\delta^{17}\text{O}$  and  $\delta^{18}\text{O}$  of terrestrial silicate minerals<sup>37,39</sup>. Samples were loaded in a Sharp reaction chamber (ref. 40). Successive, repeated blanks with  $\text{BrF}_5$  and vacuum pumping were carried out for 12 h until there was less than 150  $\mu\text{m}$  of non-condensable gas pressure remaining after a blank run. Quantitative release of oxygen by fluorination reaction was performed by heating samples individually with a  $\text{CO}_2$  laser in the presence of  $\text{BrF}_5$ . Standardization of delta values was achieved by comparison with the Gore Mountain garnet standard, USNM 107144, analysed during every analytical session.

34. Day, J. M. D. *et al.* Comparative petrology, geochemistry, and petrogenesis of evolved, low-Ti mare basalt meteorites from the LaPaz Icefield, Antarctica. *Geochim. Cosmochim. Acta* **70**, 1581–1600 (2006).
35. Baker, J., Peate, D., Waight, T. & Meyzen, C. Pb isotopic analysis of standards and samples using a  $^{207}\text{Pb}$ – $^{204}\text{Pb}$  double spike and thallium to correct for mass bias with a double-focusing MC-ICP-MS. *Chem. Geol.* **211**, 275–303 (2004).
36. Ludwig, K. R. Isoplot. Program and documentation, version 2.95. (Revised edition of US Open-File report, 91-445, 2003).
37. Rumble, D., Miller, M. F., Franchi, I. A. & Greenwood, R. C. Oxygen three-isotope fractionation lines in terrestrial silicate minerals: An inter-laboratory comparison of hydrothermal quartz and eclogitic garnet. *Geochim. Cosmochim. Acta* **71**, 3592–3600 (2007).
38. Clayton, R. N. & Mayeda, T. K. Oxygen isotope studies of achondrites. *Geochim. Cosmochim. Acta* **60**, 1999–2017 (1996).
39. Miller, M. F. Isotopic fractionation and the quantification of  $^{17}\text{O}$  anomalies in the oxygen three-isotope system: an appraisal and geochemical significance. *Geochim. Cosmochim. Acta* **66**, 1881–1889 (2002).
40. Sharp, Z. D. A laser-based microanalytical method for the *in situ* determination of oxygen isotope ratios of silicates and oxides. *Geochim. Cosmochim. Acta* **54**, 1353–1357 (1990).